



<b>Publication Year</b>	2015
<b>Acceptance in OA @INAF</b>	2021-02-23T11:10:49Z
<b>Title</b>	The effect of diamagnetic drift on motion of the dayside magnetopause reconnection line
<b>Authors</b>	Trenchi, L.; MARCUCCI, Maria Federica; Fear, R. C.
<b>DOI</b>	10.1002/2015GL065213
<b>Handle</b>	<a href="http://hdl.handle.net/20.500.12386/30551">http://hdl.handle.net/20.500.12386/30551</a>
<b>Journal</b>	GEOPHYSICAL RESEARCH LETTERS
<b>Number</b>	42

**<sub>1</sub> The effect of diamagnetic drift on motion of the**  
**<sub>2</sub> dayside magnetopause reconnection line**

L. Trenchi<sup>1</sup>, M. F. Marcucci<sup>2</sup> and R. C. Fear<sup>1</sup>

---

<sup>1</sup>School of Physics and Astronomy,  
University of Southampton, Southampton,  
UK.

<sup>2</sup>INAF - Istituto di Astrofisica e  
Planetologia Spaziali, Rome, Italy.

3 Magnetic reconnection at the magnetopause occurs with a large density  
4 asymmetry and for a large range of magnetic shears. In these conditions, a  
5 motion of the X-line has been predicted in the direction of the electron dia-  
6 magnetic drift. When this motion is super-Alfvenic, reconnection should be  
7 suppressed. We analysed a large dataset of Double Star TC-1 dayside mag-  
8 netopause crossings, which includes reconnection and non-reconnection events.  
9 Moreover, it also includes several events during which TC-1 is near the X-  
10 line. With these close events we verified the diamagnetic suppression con-  
11 dition with local observations near the X-line. Moreover, with the same close  
12 events we also studied the motion of the X-line along the magnetopause. It  
13 is found that, when reconnection is not suppressed, the X-line moves north-  
14 ward or southward according to the orientation of the guide-field, which is  
15 related to the interplanetary magnetic field  $B_Y$  component, in agreement with  
16 the diamagnetic drift.

## 1. Introduction

Magnetic reconnection between the interplanetary magnetic field (IMF) and the geomagnetic field is the main process that allows the transfer of solar wind mass, energy, and momentum into the Earth's magnetosphere. One of the most important controlling factors for magnetic reconnection at the magnetopause is the orientation of the IMF; for pure northward IMF antiparallel reconnection occurs at the high-latitude magnetopause poleward of the cusps; when the IMF is southward and/or has a large  $B_Y$  component, reconnection occurs at the dayside equatorial magnetopause. In this region several observations have shown that the orientation of the X-line is related to the sign of the  $B_Y$  component, as predicted by the component merging model [Sonnerup, 1974; Gonzales & Mozer, 1974]. It is found that reconnection at the dayside magnetopause can occur also when the local magnetic shear angle is quite low ( $90^\circ$  or less), i.e. in presence of a strong guide field [Scurry & Russell, 1994; Phan & Paschmann, 1996; Trenchi et al., 2008].

In these low shear conditions, according to the simulations of Swisdak et al. [2003] the X-line should experience a motion along the magnetopause due to the diamagnetic drift of ions and electrons. If this X-line motion exceeds the local Alfvén speed, reconnection is suppressed. Swisdak et al. [2010] proposed that reconnection is suppressed based on the local conditions at the X-line, if:

$$\Delta\beta > 2\frac{L_p}{d_i}\tan\left(\frac{\theta}{2}\right) \quad (1)$$

Where  $\Delta\beta$  is the  $\beta$  difference across the current sheet,  $\theta$  the magnetic shear angle, and  $\frac{L_p}{d_i}$  is the pressure scale length in units of ion inertial length. At the dayside magnetopause,

near the magnetic equator where the X-line is expected to lie [Trattner et al., 2007],  $\frac{L_p}{d_i}$  should be approximately equal to unity [Berchem & Russell, 1982]. With this assumption, equation 1 becomes  $\Delta\beta > 2 \tan\left(\frac{\theta}{2}\right)$ . When this equation is satisfied, reconnection should be suppressed by diamagnetic drift.

This process can explain why reconnection events are more often observed when the  $\beta$  values in the adjacent magnetosheath are lower [Paschmann et al., 1986; Scurry & Russell, 1994; Phan & Paschmann, 1996; Trenchi et al., 2008]. Indeed, the magnetopause crossings without reconnection signatures (non-reconnection events) recently examined by Phan et al. [2013] generally satisfy the equation 1, while the opposite inequality usually held for reconnection events. This process can also be important in the magnetopause of other planets [Masters et al., 2012; DiBraccio et al., 2013].

In this paper, we analyzed a large dataset (207) of Double Star TC-1 magnetopause crossings [Trenchi et al., 2008], which comprise both non-reconnection and reconnection events. We verify the results of Phan et al. [2013], that the reconnection and non-reconnection events are well-ordered by the Swisdak et al. [2010] relation. However, while in previous studies the suppression condition was evaluated on the expectation that the X-line was not too far away from the spacecraft, here we test the condition with the local conditions at the X-line by separately considering a subset of events during which TC-1 observes a reversal in the jet direction, indicating that TC-1 was very close to the X-line.

Moreover, the main result of our paper is that by considering the latter subset, we are able to demonstrate statistically that the motion of the X-line along the magnetopause is controlled by the orientation of the guide-field. This verifies a second prediction made

by Swisdak et al. [2010]; in their simulation, when the local  $\Delta\beta$  and  $\theta$  are in the non-suppressed regime, the X-line moves in the direction of the diamagnetic drift of electrons. Since the pressure gradient at the dayside magnetopause is directed outward, this results in the motion of the X-line being controlled by the orientation of the guide field, i.e. by the  $B_Y$  GSM component of the IMF.

## 2. The Double Star TC-1 dataset

This Double Star TC-1 dataset, first examined to study the occurrence of reconnection at the magnetopause, comprises all the dayside magnetopause crossings observed by TC-1 during the first year of the mission [Trenchi et al., 2008, 2009]. It is based on the plasma moments computed onboard from the Hot Ion Analyzer (HIA) [Rème et al., 2005] and magnetic field data measured by the Fluxgate Magnetometer (FGM) [Carr et al., 2005], both with four second time resolution.

In order to identify the reconnection events, we used the Walén relation and, as an example, we show an inbound magnetopause crossing in Figure 1. The first four panels display the ion density, velocity and temperatures and the magnetic field vector. For each data point in this time interval, we compared the observed velocity jump relative to a reference value in the magnetosheath ( $V - V_{MSH}$ ) with the expected velocity jump predicted by the Walén relation (Equation (1) of Trenchi et al. [2008]). The magnetosheath reference period is indicated by yellow shading. Comparing these two vectors, we obtained the two parameters used to evaluate the agreement of the Walén relation:  $R_W$  as the ratio of their absolute values and  $\Theta_W$  as their relative angle, shown in the last two panels of figure 1.

The Walén test is perfectly fulfilled when  $R_W$  equals unity and  $\Theta_W$  equals  $0^\circ$  or  $180^\circ$ , corresponding to the positive or negative signs of the Walén relation that at the dayside magnetopause correspond to observations northward or southward of the X-line. In this study we considered that the Walén relation is satisfied when  $R_W > 0.4$  and  $\Theta_W < 30^\circ$  or  $\Theta_W > 150^\circ$ , for at least three consecutive data points, with average ion density larger than  $1\text{cm}^{-3}$  [Trenchi et al., 2008]. This test indicates the presence of reconnection jets at the magnetopause or in the boundary layer. These criteria are meaningless when satisfied during magnetosheath intervals; therefore magnetosheath periods are excluded.

In this example, TC-1 crosses the magnetopause several times between 6:50 and 07:12 UT, and later it has other encounters with the boundary layer. While in the first part of the event TC-1 detects northward and dawnward jets ( $\Theta_W < 30^\circ$ , blue shadings), after 7:13 UT, it detects southward and duskward jets ( $\Theta_W > 150^\circ$ , pink shadings). This magnetopause crossing is classified as two-sided reconnection event, since TC-1 passes from northward to southward of the reconnection X-line, indicating it is very close to the spacecraft.

On the contrary, during other magnetopause crossings, called one-sided reconnection events, TC-1 detects reconnection jets that satisfy the Walén relation, but it remains on the same side of the X-line. Finally, during the non-reconnection events, no reconnection jet that satisfies the Walén relation is observed during the entire crossing. Overall, this database consists of 110 one-sided reconnection events, 33 two-sided reconnection events and 64 non-reconnection events, whose positions are shown in figure 2A, in the  $Y - Z_{GSM}$  plane.

### 3. Diamagnetic suppression of magnetic reconnection

For each of the TC-1 crossings, we identified a reference in the magnetosheath and another in the magnetosphere, both adjacent to the magnetopause, where we evaluated the average values of the ion pressure (as the trace of the pressure tensor measured by HIA) and the average magnetic field vectors. The plasma  $\beta$  in the Swisdak equation is the total  $\beta$  that includes both the ion and the electron pressures. However, the dayside magnetosheath is characterized by a large ion-to-electron temperature ratio ( $\frac{T_i}{T_e}$ ), in the range 6-12 [Paschmann et al., 1993; Phan et al., 1994]. The same large ( $\frac{T_i}{T_e}$ ) is also expected in the boundary layer, since it is related to the one in the adjacent magnetosheath [Lavraud et al., 2009]. Assuming quasi-neutrality, the ion and electron densities should be very similar. Therefore, it is expected that the ion pressure dominates over the electron pressure in these regions. For this reason, we evaluated the average total  $\beta$  from the ion pressure, assuming that the electron pressures are one eighth of the proton pressures on both sides of the magnetopause.

As expected, in the majority of cases (97%) the local  $\beta$  in the magnetosheath (MSH) is larger than the local  $\beta$  in the adjacent magnetosphere (MSPH). The few events with  $\beta_{MSH} < \beta_{MSPH}$  (7/207), are characterized by a lower magnetic field magnitude in the magnetosphere with respect to the one in the magnetosheath, while the plasma pressure in the magnetosheath is always larger than the one in magnetosphere.

Figure 2B shows the scatter plot of the magnetic shear angle ( $\theta$ ) as a function of  $|\Delta\beta|$  for the three families of events, where  $\theta$  is the angle between the magnetosheath and magnetospheric reference magnetic fields. The black lines report the theoretical prediction



given by equation 1, in the hypothesis that  $\frac{L_p}{d_i}$  is equal to 1 (continuous line) or 0.5 or 2 (dashed lines). These curves define the two regions of the  $\theta - |\Delta\beta|$  plane where reconnection should be suppressed (on the right), or where reconnection is possible since it is not suppressed by the diamagnetic drift (on the left).

If we look at the non-reconnection events, they are spread across the suppressed and non-suppressed regions. On the other hand, the majority of the reconnection events lie in the region where reconnection is not suppressed, satisfying quite well the Swisdak prediction. Considering the continuous line (1 ion inertial length thickness), 99/110 of the one-sided reconnection events are in the non-suppressed region, i.e. 10% fall in the suppressed region. This is a similar proportion to that found by Phan et al. [2013]. However, if we restrict our analysis to the two-sided reconnection events, for which we can be confident that the spacecraft is near the X-line and hence the observed conditions are more representative of the conditions at the X-line, all but one of the events (32/33) is in the non-suppressed region. Therefore, the fraction of reconnection events in the suppressed region is only 3% (1 event).

The presence of non-reconnection events in the region where reconnection should not be suppressed by diamagnetic drift could indicate that another mechanism, for example velocity shear [Cassak & Otto, 2011], turned off reconnection at the dayside magnetopause. Alternatively, pulsed reconnection may have been occurring [Trattner et al., 2015], causing the reconnection jet to be missed when TC-1 crossed the magnetopause.

On the other hand, the one-sided reconnection events in the suppressed region are not necessary at odds with the Swisdak predictions: these reconnection events could

be observed several Earth radii away from the X-line. Taking into account the magnetic shear variations along the magnetopause caused by magnetic field draping, the local shear obtained for these one-sided events could differ significantly from the shear at the X-line. Moreover, according to the maximum shear model [Trattner et al., 2007], the X-line follows the position of the local maximum of the shear angle at each local time. In this case, any displacement from the X-line would result in the underestimation of shear angle at the X-line, which could explain the local  $\theta - |\Delta\beta|$  values in the suppressed region.

Another feature that can be noted in figure 2B is that, while several one-sided reconnection events have very low  $|\Delta\beta|$ , the two-sided reconnection events have all  $|\Delta\beta| > 0.1$ , being more concentrated near the theoretical suppression condition of Swisdak. According to the diamagnetic drift effect, the X-line velocity increases as the suppression condition is approached, and, a larger X-line velocity could explain the passage of the spacecraft from one to the other side of the X-line during these two-sided events. This suggests that the diamagnetic drift has a role for the motion of the X-line when reconnection is not suppressed. In the following section, we use a subset of two-sided reconnection events to study the X-line motion along the magnetopause.

#### 4. The motion of the X-line along the dayside magnetopause

According to the Swisdak simulations, the X-line should move along the current sheet in the direction of the diamagnetic drift of the electrons. The X-line velocity with respect to the ion rest frame is given by the sum of the ion and electron diamagnetic drift:

$$V_{XLdrift} = c \frac{\nabla p_i \times \vec{B}_g}{|q_i| n_i B_g^2} + c \frac{\nabla p_e \times \vec{B}_g}{|q_e| n_e B_g^2} \quad (2)$$

where  $c$  is the speed of light,  $\vec{B}_g$  is the guide field at the center of the current sheet, while  $p_i$  and  $p_e$ ,  $q_i$  and  $q_e$ ,  $n_i$  and  $n_e$  are the pressures, charges and densities of ions and electrons, respectively. At the dayside magnetopause, where the pressure gradient is outward along the magnetopause normal, the direction of the X-line motion is related to the orientation of the guide field, which is mainly determined by the  $B_Y$  component of the IMF. Therefore the X-line is expected to move northward/southward for duskward/dawnward guide fields respectively.

The guide field can be evaluated as the projection of the magnetosheath or magnetospheric field along the X-line. For the two-sided reconnection events, we evaluated the orientation of the X-line predicted by the component merging model [Sonnerup, 1974; Gonzales & Mozer, 1974] from the magnetosheath and magnetospheric fields, which are likely to be similar to the fields at the reconnection site. Here we introduce a local reference frame, with  $\widehat{N}$  along the Fairfield magnetopause normal [Fairfield, 1971],  $\widehat{XL}$  along the X-line orientation with a positive  $Y_{GSM}$  component and  $\widehat{RC}$  (representing the reconnecting component), perpendicular to these vectors, with a positive  $Z_{GSM}$  component (see figure 3). The X-line orientation is obtained as perpendicular to  $\vec{B}_{MSH} - \vec{B}_{MSPH}$ , where  $\vec{B}_{MSH}$  and  $\vec{B}_{MSPH}$  are the projections in the plane perpendicular to the Fairfield normal of the magnetosheath and magnetospheric fields, respectively.

For several two-sided reconnection events, a single passage from northward to southward jets, or vice versa, is observed during the entire crossing, such as in the example shown in figure 1. In these single passage events we can make the simplifying assumption that the X-line velocity does not change direction during the event. On the contrary, other two-

sided events are characterized by multiple passages between northward and southward jets. This could be due to the presence of multiple X-lines, which could eventually move in the same direction, or alternatively to a reversal of the X-line motion. In the former case, the formation of FTEs between the multiple X-lines is expected [Lee & Fu, 1985; Raeder, 2006; Trenchi et al., 2011; Fear et al., 2012a, b].

In figure 2B, the black bars over the cyan dots indicate the two-sided single passage events. It is interesting to note that all the two-sided events with low magnetic shear ( $\theta < 90^\circ$ ) are characterized by a single passage. In figure 4A we report the distribution of the magnitude of  $\vec{B}_g$  for single passage and multiple passage events. In agreement with their lower magnetic shear, the single passage events have a much stronger guide field compared with the multiple passage events. The average values are  $|\vec{B}_g| = 26 \pm 15nT$  and  $|\vec{B}_g| = 6 \pm 5nT$  for the single passage and multiple passage events, respectively. According to equation 2, a higher guide field would produce a larger X-line velocity, which could be responsible for the clear constant motion of the X-line in one direction during these single passage events.

The direction of the X-line motion can be easily inferred for the single passage events from the order in which northward and southward reconnection jets are observed. When first northward and then southward reconnection jets are detected, the X-line is moving northward with respect to the spacecraft, while it is moving southward when the order of the reconnection jets is the opposite. In figure 4B,  $B_g$  as a function of the order in which the jets are detected for the single passage events is reported. The blue dots indicate

the northward-southward events (N-S), while the red dots are the southward-northward events (S-N).

Our observations show a good agreement with the diamagnetic motion of the X-line: all the S-N events have a negative  $B_g$ , and all but one of the N-S events have a positive  $B_g$ . The only N-S event with a negative guide field still has a  $B_g$  very close to zero ( $-0.4nT$ ). These observations suggest therefore that the diamagnetic drift has a role in the X-line motion along the magnetopause when the local conditions are not in the suppressed region, as predicted by the simulations of Swisdak et al. [2003]. We also verified that using other X-line models [Moore et al., 2002; Swisdak & Drake, 2007; Borovsky, 2013] the orientation of the guide field  $B_Y$  component do not change. Therefore, the choice of a different X-line model would not change our findings.

The other mechanism that could be responsible for the X-line motion is the convection from the adjacent magnetosheath. Indeed, a recent study found that during a reconnection event at high latitude characterized by super-Alfvenic magnetosheath velocity, the X-line was moving tailward convected by the magnetosheath velocity [Wilder et al., 2014]. We therefore evaluated the component of the magnetosheath velocity perpendicular to the X-line ( $V_{MSHRC}$ ), which is the component that could convect the X-line. If the X-line motion is related to the magnetosheath convection, since the RC axis has a positive  $Z_{GSM}$  component, N-S events should be associated with positive  $V_{MSHRC}$  while S-N events with negative  $V_{MSHRC}$ . We also estimated the X-line diamagnetic drift velocity predicted by the Swisdak simulation with equation 2). As for the suppression condition, we assumed

that the electron pressures are one eighth of the proton pressures on both sides of the magnetopause and  $\frac{L_p}{d_i}$  is equal to 1. The X-line velocity is therefore obtained as:

$$V_{XLdrift} = c \frac{9}{8} \frac{(p_{MSH} - p_{MSPH}) B_g}{d_i |q_i| n_i B_g^2} \hat{R}C \quad (3)$$

where  $p_{MSH}$  and  $p_{MSPH}$  are the average proton pressures in magnetosheath and magnetospheric reference, respectively. While these assumptions can certainly introduce errors in the values of  $V_{XLdrift}$ , we believe that it can not change its sign, since outward pressure gradient at the magnetopause implies that  $p_{MSH} > p_{MSPH}$ .

In figure 4C,  $V_{XLdrift}$  as a function of  $V_{MSHRC}$  is reported. Blue and red dots refer to N-S and S-N events, for which the velocity of the X-line is northward and southward respectively.  $V_{XLdrift}$  better separates the N-S from the S-N events. Indeed, all the S-N events are associated with negative  $V_{XLdrift}$  and all but one of the N-S events are associated with positive  $V_{XLdrift}$ . On the contrary, five of the N-S events are observed during negative  $V_{MSHRC}$ , contrary to expectation according to the magnetosheath convection. Therefore, it seems that the velocity of the adjacent magnetosheath does not affect the motion of the X-line at the dayside magnetopause. However it is interesting to note that the only event not in agreement with the diamagnetic drift, the only N-S event with negative  $V_{XLdrift}$ , is the only event with  $V_{MSHRC}$  larger than Alfvén magnetosheath velocity. In this case, the magnetosheath convection hypothesis is in agreement with the order of the jets.

## 5. Summary and Conclusions

During component reconnection, the diamagnetic drift of ions and electrons causes a motion of the X-line along the dayside magnetopause, which is proportional to the local

pressure gradient and to the intensity of the guide field at the X-line [Swisdak et al., 2003].

If this X-line velocity exceeds the local Alfvén speed, reconnection is suppressed.

In order to investigate the effects of diamagnetic drift, we analysed a large dataset of Double Star TC-1 magnetopause crossings (207) which includes both reconnection events and magnetopause crossings without reconnection signatures. The reconnection events were divided into two categories, one where the distance of the spacecraft from the X-line is unknown (one-sided events, can be also several  $R_E$  from the X-line), the other one where TC-1 explores both sides of the X-line, being probably very close to the reconnection site (two-sided events). This latter category allows us to test the suppression condition with the local conditions at the X-line.

We found that most of the reconnection events were observed in the regime where reconnection is not predicted to be suppressed by diamagnetic drift. Moreover, the agreement with the suppression condition further increased when the spacecraft was near the X-line (97%, or 32/33 of the two-sided events in the non-suppressed region) with respect to the one-sided events (90% in the non-suppressed region). The fact that the local conditions at the X-line show such a good agreement with the suppression condition, confirms that the diamagnetic drift is able to turn off reconnection at the dayside magnetopause.

For several two-sided events, we also determined the direction of the X-line motion with respect to the spacecraft, from the order in which northward and southward reconnection jets were detected. With these events, we tested if the X-line motion is related to the diamagnetic drift, which should move the X-line in the direction of the electron drift even when reconnection is not suppressed [Swisdak et al., 2003]. At the magnetopause, where

the pressure gradient is outward, the direction of the X-line motion should be related to the orientation of the guide field, which is principally determined by the IMF  $B_Y$  component.

We found that the direction of the X-line motion is in agreement with the velocity predicted by the diamagnetic drift for all but one of these events (9/10), which are all characterized by a non-negligible guide field. The only event not in agreement with the diamagnetic drift prediction has instead a very small guide field, which results in a small X-line velocity. On the contrary, the convection hypothesis is not in agreement with the observations for half of these events. This suggests that, during component reconnection, the X-line has always a motion along the magnetopause under the effect of diamagnetic drift. This X-line motion, not considered by the present models that predict the X-line location, can cause a non-stationary reconnection even for stable solar wind conditions.

**Acknowledgments.** L.T. is currently supported by STFC Ernest Rutherford Grant ST/L002809/1, and R.F. is supported by STFC Ernest Rutherford Fellowship ST/K004298/1. Double Star data are available via Cluster Science Archive (<http://www.cosmos.esa.int/web/csa>). L.T. thanks M. Hesse and G. Pallocchia for the useful discussions.

## References

- Berchem, J., & Russell, C. T. 1982, The thickness of the magnetopause current layer - ISEE 1 and 2 observations, *J. Geophys. Res.*, , 87, 2108
- Borovsky, J. E. 2013, *Journal of Geophysical Research (Space Physics)*, 118, 2113



- Carr, C., , Brown, P., Zhang, T. L., Gloag, J., Horbury, T., Lucek, E., Magnes, W.,  
 O'Brien, H., Oddy, T., Auster, U., Austin, P., Aydogar, O., Balogh, A., Baumjohann,  
 W., Beek, T., Eichelberger, H., Fornacon, K.-H., Georgescu, E., Glassmeier, K.-H.,  
 Ludlam, M., Nakamura, R., and Richter, I (2005). The Double Star magnetic field  
 investigation: instrument design, performance and highlights of the first years of obser-  
 vations, *Ann. Geophys.*, *23*, 2713-2732, 2005.
- Cassak, P. A., & Otto, A. 2011, *Physics of Plasmas*, *18*, 074501.
- Dibraccio, G. A., Slavin, J. A., Boardsen, S. A., et al. 2013, *Journal of Geophysical  
 Research (Space Physics)*, *118*, 997.
- Fairfield D. H. (1971), Average and unusual locations of the Earth's magnetopause and  
 bow shock, *J. Geophys. Res.*, *76*, 6700.
- Fear, R. C., M. Palmroth and S. E. Milan, Seasonal and clock angle control of the location  
 of flux transfer event signatures at the magnetopause, *J. Geophys. Res.*, *117*, A04202,  
 doi:10.1029/2011JA017235, 2012
- Fear, R. C., S. E. Milan and K. Oksavik, Determining the axial direction of high-shear  
 flux transfer events: Implications for models of FTE structure, *J. Geophys. Res.*, *117*,  
 A09220, doi:10.1029/2012JA017831, 2012
- Gonzales, W. D. and F. S. Mozer (1974), A quantitative model from the potential resulting  
 from reconnection with an arbitrary interplanetary magnetic field, *J. Geophys. Res.*, ,  
*79*, 4186.
- Lavraud, B., Borovsky, J. E., Génot, V., et al. 2009, Tracing solar wind plasma entry into  
 the magnetosphere using ion-to-electron temperature ratio, *Geophys. Res. Lett.*, , *36*,

L18109

Lee, L. C. and Z. F. Fu (1985), A theory of magnetic flux transfer at the Earth's magnetopause, *Geophys. Res. Lett.*, *12*, No. 2, pages 105-108.

Masters, A., Eastwood, J. P., Swisdak, M., et al. 2012, *Geophys. Res. Lett.*, , 39, L08103.

Moore, T. E., Fok, M.-C., & Chandler, M. O. 2002, *Journal of Geophysical Research* (Space Physics), *107*, 1332

Paschmann G., Baumjohann W., Sckopke N., Papamastorakis I., Carlson, C. W., Sonnerup B. U. Ö. and Lühr H. (1986), The magnetopause for large magnetic shear - AMPTE/IRM observations, *J. Geophys. Res.*, *91*, 11,099-11,115.

Paschmann, G., Baumjohann, W., Sckopke, N., Phan, T.-D., & Luehr, H. Structure of the dayside magnetopause for low magnetic shear, 1993, *J. Geophys. Res.*, , 98, 13409

Phan, T.-D., Paschmann, G., Baumjohann, W., Sckopke, N., & Luehr, H. 1994, The magnetosheath region adjacent to the dayside magnetopause: AMPTE/IRM observations, *J. Geophys. Res.*, , 99, 121

Phan, T.D. and Paschmann, G., Ö. Sonnerup, (1996), Low-latitude dayside magnetopause and boundary layer for high magnetic shear 2. Occurrence of magnetic reconnection in *J. Geophys. Res.*, *101*, 7817-7828, 1996.

Phan, T. D., Paschmann, G., Gosling, J. T., et al. 2013, The dependence of magnetic reconnection on plasma and magnetic shear: Evidence from magnetopause observations, *Geophys. Res. Lett.*, , 40, 11

Raeder, J., (2006), Flux Transfer Events: 1. generation mechanism for strong southward IMF, *Ann. Geophys.*, *24*, 381-392, 2006.

- Rème, H. , Dandouras, I., Aoustin, C., Bosqued, J. M., Sauvaud, J. A., Vallat, C.,  
 Escoubet, P., Cao, J. B., Shi, J., Bavassano-Cattaneo, M. B., Parks, G. K., Carlson, C.  
 W., Pu, Z., Klecker, B., Moebius, E., Kistler, L., Korth, A., Lundin, R., and the HIA  
 team, (2005), The HIA instrument on board the Tan Ce 1 Double Star near-equatorial  
 spacecraft and its first results, *Ann. Geophys.*, *23*, 2757-2774, 2005.
- Scurry, L. and Russell, C.T., Gosling, J.T., (1994), A statistical study of accelerated flow  
 events at the dayside magnetopause, in *J. Geophys. Res.*, *99*, 14,815-14,829, 1994.
- Sonnerup, B. U. Ö. (1974), The reconnecting magnetosphere, in *Magnetospheric Physics*,  
 edited by B. M. McCormac, p. 23, D. Reidel, Dordrecht-Holland.
- Swisdak, M., Rogers, B. N., Drake, J. F., & Shay, M. A. 2003, Diamagnetic suppression  
 of component magnetic reconnection at the magnetopause *J. Geophys. Res.*, , 108, 1218
- Swisdak, M., & Drake, J. F. 2007, *Geophys. Res. Lett.*, , 34, L11106
- Swisdak, M., Opher, M., Drake, J. F., & Alouani Bibi, F. 2010, The Vector Direction of  
 the Interstellar Magnetic Field Outside the Heliosphere *Astrophys. J.*, , 710, 1769
- Trattner, K. J., Mulcock, J. S., Petrinec, S. M., & Fuselier, S. A. 2007, Probing the bound-  
 ary between antiparallel and component reconnection during southward interplanetary  
 magnetic field conditions *J. Geophys. Res.*, , 112, A08210
- Trattner, K. J., Onsager, T. G., Petrinec, S. M., & Fuselier, S. A. 2015, Journal of  
 Geophysical Research (Space Physics), 120, 1684.
- Trenchi, L., M. F. Marcucci, G. Pallochia, G. Consolini, M. B. Bavassano Cattaneo, A.  
 M. Di Lellis, H. Rème, L. Kistler, C. M. Carr, and J. B. Cao 2008, Occurrence of  
 reconnection jets at the dayside magnetopause: Double Star observations, *J. Geophys.*

*Res.*, 113, A07S10, doi:10.1029/2007JA012774.

Trenchi, L., Marcucci, M. F., Pallocchia, G., et al. 2009, Magnetic reconnection at the dayside magnetopause with Double Star Tc1 data. *Memorie della Società Astronomica Italiana*, 80, 287

Trenchi, L., Marcucci, M. F., Rème, H., Carr, C. M., & Cao, J. B. 2011, TC-1 observations of a flux rope: Generation by multiple X-line reconnection. *Journal of Geophysical Research (Space Physics)*, 116, A05202

Wilder, F. D., Eriksson, S., Trattner, K. J., et al. 2014, Observation of a retreating X-line and magnetic islands poleward of the cusp during northward interplanetary magnetic field conditions, *Journal of Geophysical Research (Space Physics)*, 119, 9643

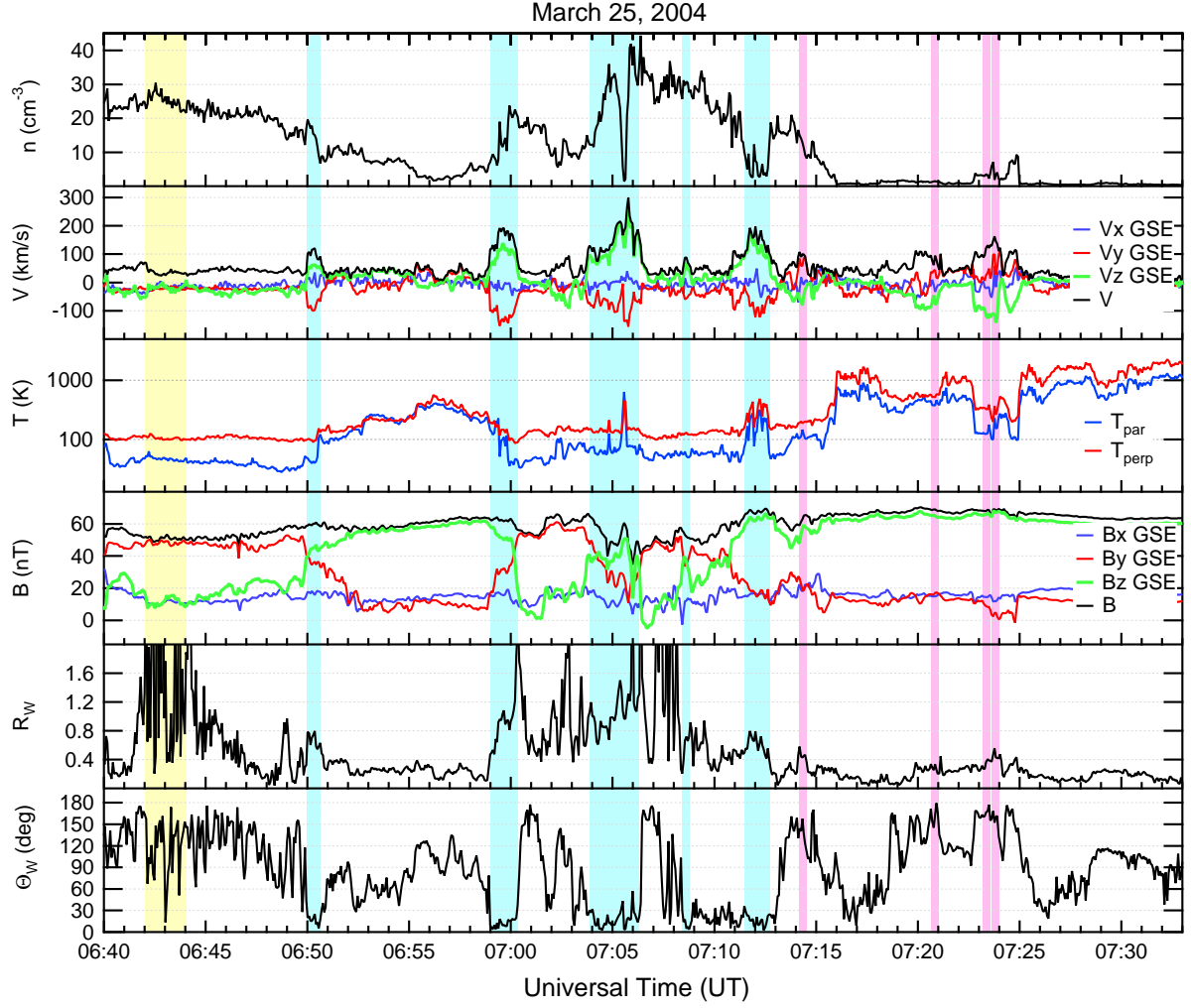


**Figure 1.** An example of magnetopause crossing with reconnection jets. In the top four panels the ion density, velocity, temperatures and the magnetic field vector. The last two panels show the parameters used to evaluate the agreement of the Walén test, that is perfectly fulfilled when  $R_W$  equals unity and  $\Theta_W$  equals  $0^\circ$  or  $180^\circ$ , corresponding to observations northward or southward of the X-line. In this event TC-1 explores both sides of the X-line, observing first northward and then southward reconnection jets, therefore it is classified as a two-sided event.

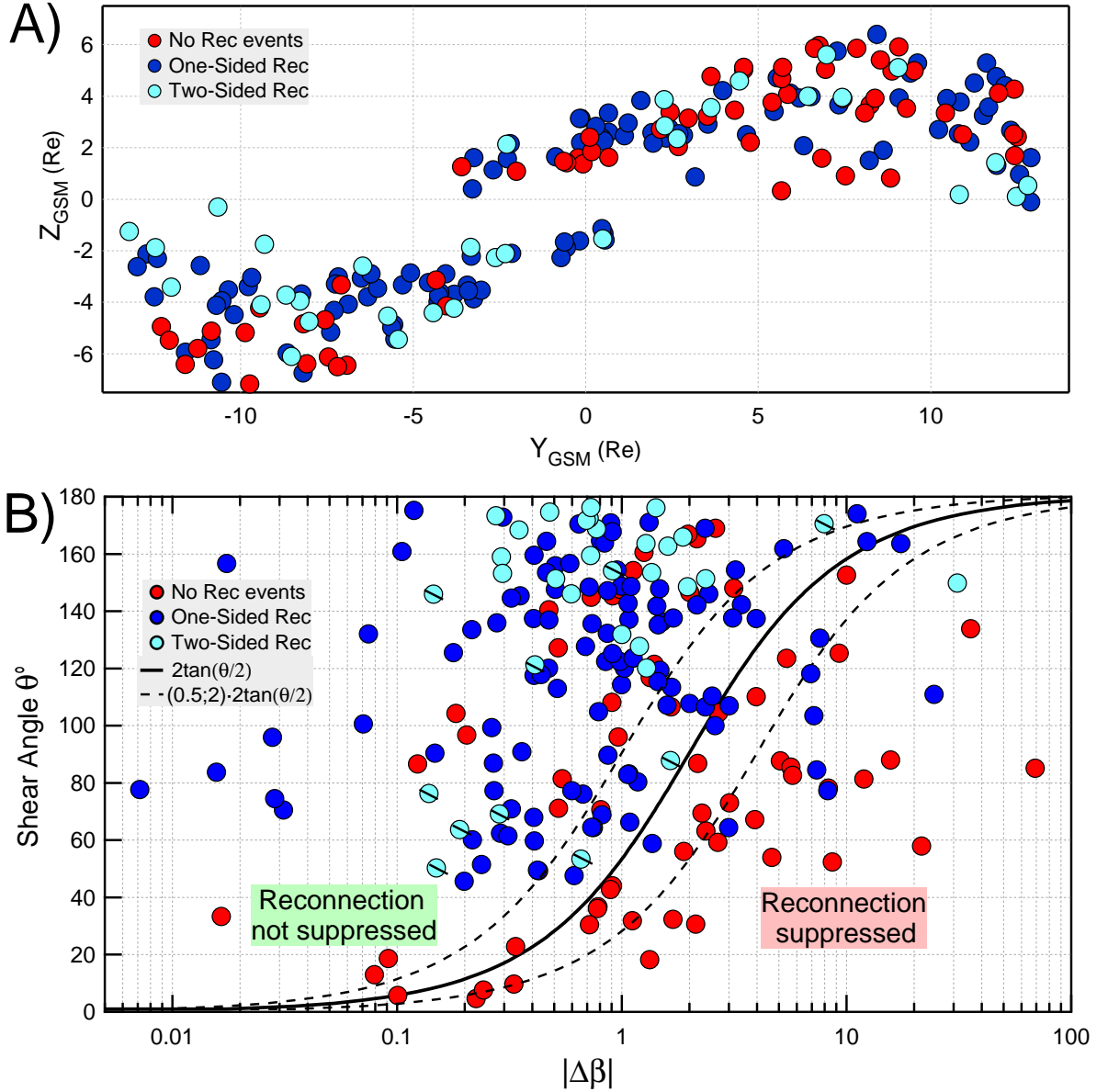


**Figure 2.** Panel A). The positions of the non-reconnection events (red dots), one-sided reconnection events (blue dots) and two-sided reconnection events (cyan dots) in the  $Y - Z_{GSM}$  plane.

Panel B). The magnetic shear angle ( $\theta$ ) as a function of  $|\Delta\beta|$  for the non-reconnection events (red dots), one-sided reconnection events (blue dots) and two-sided reconnection events (cyan dots). The black lines are the prediction for the diamagnetic suppression of reconnection (equation 1), when  $\frac{L_p}{d_i}$  is equal to 1 (continuous line) or 0.5 or 2 (dashed lines). On the right of these curves, reconnection should be suppressed by diamagnetic drift effect, while on the left it should not be suppressed.

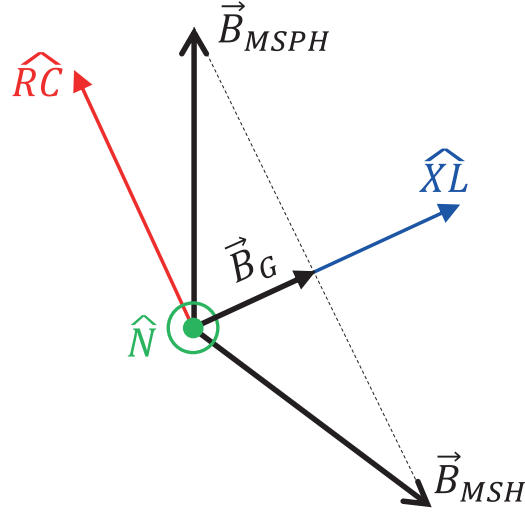


**Figure 3.** A scheme of the local X-line reference used to evaluate the guide field component ( $\vec{B}_g$ ) for the two-sided reconnection events.

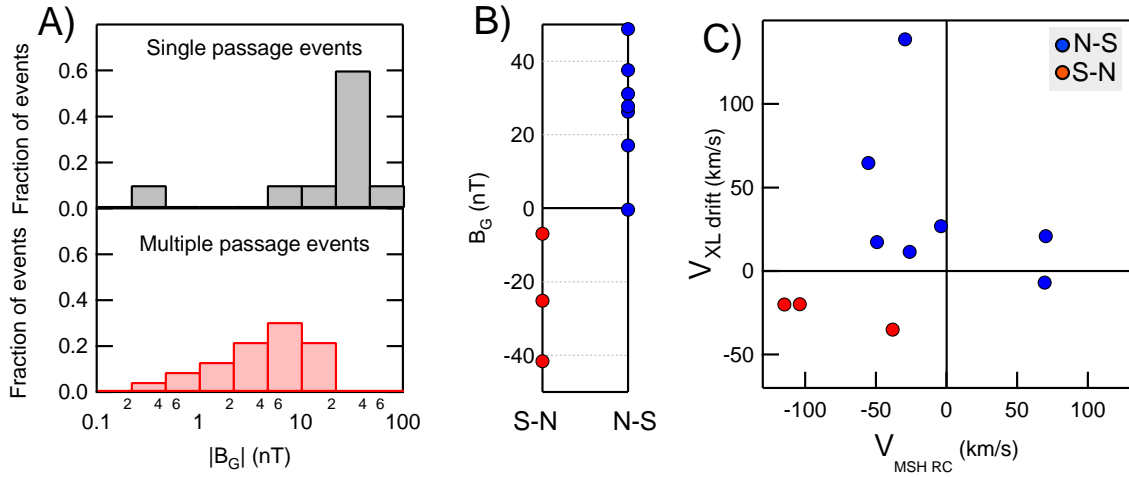


**Figure 4.** Panel A). The histograms of the magnitude of the guide field component for single passage and multiple passage events.

Panel B).  $B_g$  as a function of the order in which the jets are detected. Panel C). The diamagnetic drift velocity of the X-line as a function of the velocity of the adjacent magnetosheath perpendicular to the X-line. Blue and red dots indicate N-S and S-N events, for which the observed X-line velocity is northward and southward, respectively.